Published in final edited form as:
Neurosurgery. 2009 December ; 65(6 Suppl): 226–236. doi:10.1227/01.NEU.0000350868.95634.CA.

Preoperative Sensorimotor Mapping in Brain Tumor Patients using Spontaneous Fluctuations in Neuronal Activity Imaged with fMRI: Initial Experience

Dongyang Zhang, BA[1,*], **James M. Johnston, MD**[2], **Michael D. Fox, MD/PhD**[1], **Eric C. Leuthardt, MD**[2], **Robert L. Grubb, MD**[2], **Michael R. Chicoine, MD**[2], **Matthew D. Smyth, MD**[2], **Abraham Z. Snyder, MD/PhD**[1], **Marcus E. Raichle, MD**[1,3,4,5,6], and **Joshua S. Shimony, MD/PhD**[1]

[1] Department of Radiology, Washington University, St. Louis, Missouri

[2] Department of Neurosurgery, Washington University, St. Louis, Missouri

[3] Department of Neurology, Washington University, St. Louis, Missouri

[4] Department of Neurobiology, Washington University, St. Louis, Missouri

[5] Department of Psychology, Washington University, St. Louis, Missouriv

[6] Department of Biomedical Engineering, Washington University, St. Louis, Missouri

Abstract

Objective—To describe initial experience with resting state correlation mapping as a potential aid for presurgical planning of brain tumor resections.

Methods/Technique—Resting state blood oxygenation dependent (BOLD) fMRI was acquired in seventeen healthy young adults and four patients with brain tumors invading sensorimotor cortex. Conventional fMRI motor mapping (finger tapping protocol) was also performed in the patients. Intraoperatively, motor hand area was mapped using cortical stimulation.

Results—Robust and consistent delineation of sensorimotor cortex was obtained using the resting state BOLD data. Resting state functional mapping in patients showed localization to sensorimotor areas consistent with cortical stimulation mapping (CSM) and in all cases performed as well or better than task-based fMRI.

Conclusions—Resting state correlation mapping is a promising tool for reliable functional localization of eloquent cortex. This method compares well with “gold standard” CSM and offers several advantages in comparison to conventional motor mapping fMRI.

Keywords

brain tumor; fMRI; resting state; spontaneous fluctuations

Corresponding Authors: Dongyang Zhang, Washington University, Department of Radiology, Campus Box 8225, 510 South Kingshighway Blvd. St. Louis, MO 63110, zhangd@npg.wustl.edu, Tel: (314) 362-6907, Fax: (314) 362-6110, Joshua S. Shimony, Washington University, Department of Radiology, Campus Box 8225, 510 South Kingshighway Blvd. St. Louis, MO 63110.
*primary corresponding author

Introduction

Accurate localization of eloquent cortex enables optimal neurosurgical tumor resection and minimizes post-operative neurological deficits. Functional magnetic resonance imaging (fMRI) is a non-invasive technique for examining brain function that utilizes changes in blood oxygenation to identify areas of increased or decreased neuronal activity (33,[39]). This technique has proven to be extremely valuable in the laboratory, allowing researchers to localize the representation of sensory, motor and cognitive processes (38). Further, fMRI research has identified functional brain abnormalities in populations of patients with neurological and psychiatric disease and has contributed to the investigation of drug treatment effects. Despite its success in research, fMRI is just beginning to make the transition to the clinic as a tool for obtaining important diagnostic or prognostic information in individual patients (35). This transition has encountered many challenges and, while promising, the clinical utility of fMRI has yet to be firmly established.

Perhaps the area showing the greatest promise is pre-operative functional brain mapping to help guide neurosurgical planning (24,[35,46]). This is used most often to identify brain areas used in movement and language so that these areas can be avoided during cortical tumor or epilepsy resections, but it has also been combined with EEG to identify foci of epileptic activity (32). Functional foci identified using fMRI have been shown to correlate well with foci identified using more invasive techniques such as intra-operative electrophysiology (46) and Wada testing (1,[5]). Further, the distance from an fMRI-identified functional region to the surgical margin has been shown to correlate with loss of function post-operatively (24). Finally, when made available, pre-surgical functional information from fMRI is mentioned in approximately 75% of patient's neurosurgery notes, though the utilization of this information for medical planning is unknown (24). Despite the evidence suggesting that fMRI can identify functional brain regions in individual patients and its use in pre-operative planning, it is far from optimized. Moreover, improved patient outcome has yet to be demonstrated.

One of the reasons it has been difficult to demonstrate a clear clinical benefit of pre-operative fMRI is that there are limitations to its use and obstacles preventing fMRI from being clinically effective (46). For example, pre-operative localization is only as good as the patient's ability to perform the task or function one is attempting to localize. A major problem is that patient's task performance is often impaired, rendering localization as well as comparison with normal controls difficult or impossible (37). Since patients must be awake to perform tasks, anesthesia cannot be used and patient movement may become a significant problem (31). In many cases, clinical fMRI cannot be performed at all. Finally, task-related modulations in the fMRI signal are often small relative to large background fluctuations or “fMRI noise” requiring that subjects perform a task repeatedly so that results may be averaged and a suitable image obtained.

A recent advance that can address several of the limitations of pre-operative fMRI mapping is the use of spontaneous blood oxygen level dependent (BOLD) fluctuations to identify functionally related regions (17). Instead of examining changes in blood oxygenation associated with a task, one can simply examine the spontaneous modulations in the BOLD signal while subjects rest quietly in the scanner. Spontaneous BOLD fluctuations are not random noise, but rather fluctuations in neuronal activity that are correlated within distinct functional networks (17). For example, strong coherence is reproducibly present between the left and right sensorimotor cortices (6,[11,12,14,20,34,47]) and between language areas (11,[27]) even in the “resting state,” i.e., in the absence of imposed task performance. Thus, using spontaneous activity one can generate resting state correlation maps that characteristically replicate the topography of task-related fMRI (17).

There are several advantages of using resting state activity for preoperative mapping. First, subjects need not perform a task. Hence, mapping can proceed despite cognitive dysfunction, physical handicap, or young age. Second, all brain systems can be studied using the same data. This is in contrast to task activations which require dedicated data acquisitions for each function one is attempting to localize. Because one can use the same set of data, signal to noise can be improved and acquisition times reduced. Third, spontaneous activity continues when subjects are asleep (21,[28]) or anaesthetized (30,[36],[44]). Acquisitions under these conditions can be used in patients unable to remain still in an MR scanner.

However, before the clinical utility of resting state correlation mapping can be demonstrated, one must first establish that this method is capable of generating consistent maps within single individuals. In this study we will assess reliability by means of repeated acquisitions within the same individual. Then we will demonstrate the utility of resting state mapping in a neurosurgical setting with comparison to task-based fMRI and intra-operative stimulation mapping.

Methods

Subjects and fMRI Data Acquisition

A total of 21 subjects participated in this study (17 normal controls and 4 patients with brain tumors). All clinical and experimental protocols were approved by the Human Research Protection Office at Washington University School of Medicine.

To demonstrate the normal pattern of neuroanatomical networks observed with resting state correlation mapping, imaging data previously acquired (19) in 17 healthy young adults were analyzed at the individual and group level. All subjects were scanned using BOLD sensitized fMRI (4 × 4 × 4 mm voxels, TE 25 msec, TR 2.16 sec) on a 3T Siemens (Erlangen, Germany) Allegra MR scanner and included four 7 minute runs of 194 frames (28 minutes total) per subject during which subjects visually fixated on a cross-hair. No task was imposed except to remain still and not fall asleep.

Four patients with brain tumors invading motor and sensory cortices were scanned prior to surgical resection using a resting state protocol nearly identical to above (visual fixation to crosshairs, 4 × 4 × 4 mm voxels, TE 27 msec, TR 2.2 sec, 820 frames for a total of 30 min on a 3T Siemens Trio MR scanner). Both healthy and patient populations completed structural imaging that was used for atlas transformation including a T1-weighted MP-RAGE and a T2 weighted (T2W) fast spin echo scan.

In addition, the patient population was also scanned while performing a motor task using a standard clinical fMRI protocol (block design bilateral finger-tapping, alternating each finger with the thumb, 30 seconds rest, 30 seconds task, repeated 4 times for a total of 4 minutes, 4 × 4 mm in-plane resolution, 3 mm slice thickness, TE 25 msec, TR 3 sec) on a 3T Siemens Trio MR scanner.

Preprocessing of Imaging Data

Resting state and task-evoked BOLD fMRI data were preprocessed according to previously published methods standard to all of our BOLD fMRI data (50). Voxels corresponding to mass lesions were excluded (by masking) from the computations during registration of the T1-weighted structural images to the atlas representative template. Additional preprocessing steps described below only applied to the resting state data. Low-pass filtering was employed to retain frequencies below 0.1Hz (12). No high-pass filter was used. Spurious variance due to head motion was removed by first calculating the six parameters resulting from rigid body correction and then regressing these time courses along with their first derivatives.

Seed-based Correlation Mapping

Seed-based correlation maps were generated by extracting the BOLD fMRI time course from spherical seed regions of interest (6mm radius). The Pearson product-moment correlation coefficient then was computed between regional time courses and every voxel in the brain. Resting state correlation mapping in patients was performed by placing seeds in morphologically normal cortical tissue in the hemisphere contralateral to the tumor. Anatomical coordinates for seed-based mapping were derived as follows. The left sensorimotor cortex Talairach coordinate (-39, -26, 51) was used as the standardized seed region in all healthy controls and in all clinical cases except Case 3 (Figures 1,2B,3A,4B,6B). This coordinate was calculated as the center of mass from a group of 14 subjects performing button press responses (20, [48]). The right intraparietal sulcus (IPS) coordinate (25,-58,52) (Figure 5E) was derived as a peak foci from a group of 10 subjects during the investigation of anticorrelations in resting state neuronal activity (18). This region of the brain exhibits increases in activity during externally cued attention and working memory tasks (9). In Case 3, the coordinate of the seed in right sensorimotor cortex was determined empirically by shifting placement of the seed from the standardized coordinate until the normal spatial pattern of the sensorimotor network was seen. This coordinate (34.5,-6,54) (Figure 5C) was determined to be approximately 20mm anterior to the peak foci of the right sensorimotor cortex in the same group of 14 healthy young adults discussed above (coordinates 38,-26,48) (20).

Seed-based correlation maps were further processed as follows. Correlation coefficients were converted to an approximately normal distribution using Fisher's *r*-to-*z* transform. Bartlett correction was applied before *z*-transformed correlation values were converted to Z scores (50). Population level maps (Figure 1A) were generated using random effects analysis (two tailed, equal variance) across all subjects. For display purposes, voxel boundaries were smoothed using fourfold interpolation and then displayed using in-house software written on the MATLAB platform (The MathWorks; Natick, MA). Thresholding was determined by neuroradiologist JSS based on qualitative evaluation to best demonstrate functional neuronal activity while minimizing spatially non-specific noise that is likely of non-neuronal origin.

Partial correlation, which was used for separation of sensory and motor activity, was implemented according to the methods of referenced work (50). Spherical 6mm radius ROIs were manually defined to include voxels only in either motor or sensory cortex (Talairach coordinates: -45, -9, 51; -48, -25, 51, respectively).

Independent Component Analysis

Blind source separation using independent component analysis (ICA) was performed on resting state data preprocessed up to and including the bandpass stage (see above). ICA decomposition was performed using Multivariate Exploratory Linear Optimized Decomposition into Independent Components (MELODIC v3.0) as part of the Oxford Centre for Functional Magnetic Resonance Imaging of the Brain Software Library package (FMRIB, Oxford U.K.; FSL v4.1)(3,[42]). Registration and bandpassing were not performed in MELODIC. Automatic dimensionality estimate was performed before running single-session ICA analysis.

Mapping of Task-Based fMRI Activity

Processing steps standard to generation of task-evoked activation maps were used in the present analysis. The waveform corresponding to task performance was convolved with a hemodynamic function of the gamma type (8) and then entered into a general linear model to identify on a voxelwise basis regions of the brain correlated with task performance. To maintain consistency of preprocessing procedures between task-based and resting state mapping, additional processing steps were employed though they do not affect the interpretation of the

results. These steps include Fisher's *r*-to-*z* transform and conversion to Z scores after correcting for the number of independent frames according to Bartlett's theory (see above).

Intra-operative Cortical Stimulation Mapping

Cortical stimulation was performed using a 60Hz biphasic square wave Ojemann stimulator (Integra Radionics, Burlington MA) with a 1.25ms peak pulse duration. Injected current started at 2mA and increased in steps of 2mA until a minimal twitching of the contralateral hand was observed. Electrical current threshold never exceeded 16mA peak-to-peak and typically were less than 10mA. Cortical stimulation mapping (CSM) data were available in 3 of the 4 cases. Stereotactic coordinates were recorded on a neuronavigation system (StealthStation TREON plus, Medtronic, Louisville, KY) for Cases 3,4 and intraoperative photos of labeled cortical stimulation points were available for Case 1. Based on the anatomic location of sulci and gyri relative to the site of cortical stimulation, we estimated the cortical stimulation points for presentation in Figures 2A, 5A, and 6A.

Results

Resting state fMRI scans acquired in a group of 17 healthy young adults show the distribution of the sensorimotor system in normal individuals. By placing a seed in the hand region of the left sensorimotor cortex, the correlation of resting state activity between this reference point and every other area of the brain was mapped (Figure 1A). Correlations were seen locally around the seed as well as in homotopic contralateral hemisphere, but were spatially specific to the sensorimotor system and do not spread to neighboring areas of the brain. Next the consistency of this method was tested at the individual subject level by comparing maps generated for each of four repeat scans (7 minutes each). Using the same seed region as above, robust and consistent patterns of correlated activity were seen in each of the repeated trials, shown in Figure 1B for two of the seventeen individuals. A grouping of our results into two categories, within subject and across subject comparisons, revealed a greater similarity of resting state maps generated within an individual than across individuals ($p<8.4\times10^{-56}$ Wilcoxon rank-sum test on the z-transformed spatial correlation coefficient between two maps).

Patients with brain tumors invading the somatosensory cortex (Table 1) were imaged using resting state fMRI as well as task-based fMRI (see Methods). The seed region used above in the controls served as a standardized seed for generation of sensorimotor correlation maps in all of cases presented below except Case 3. All patients subsequently underwent tumor resection.

Case 1

A 57-year-old male presented with unsteadiness of left upper and lower extremities as well as progressive sensory loss in his left lower extremity. Structural MRI showed an intracranial mass in the right parietal cortex extending anteriorly near the central sulcus (Figure 2A).

Subsequent to structural MR, resting state fMRI scans were performed to functionally identify the sensorimotor cortex near the tumor mass. Since neuronal activity within neuroanatomical networks are correlated even in the resting state (7), seeding the sensorimotor cortex of the left hemisphere generated correlations that localized to the contralateral sensorimotor cortex. Figure 2B shows the correlation map using a seed in the morphologically normal left sensorimotor cortex (blue circle). Spatial asymmetry of functional activity is evident. The left hemisphere showed localization very similar to healthy individuals, while activity ipsilateral to the tumor was shifted antero-laterally suggesting displacement of cortical tissue involved in sensorimotor function. Intraoperative somatosensory evoked potential mapping identified a

central sulcus displaced anteriorly to the tumor, while CSM identified the hand region to be anterior to the displaced central sulcus (Figure 2, green circle), consistent with resting state observations of brain shift due to intracranial mass compression.

An important feature of resting state correlation mapping in healthy subjects is the consistency of functional maps generated with this technique, as presented earlier. To test the consistency in this tumor patient, we divided the fMRI data into halves, comparing the functional map generated from the first 15 minutes and the last 15 minutes. Figure 3A shows evident similarity of these two maps.

In addition, two trials of task-based fMRI were collected using the standard task-based fMRI protocol in which the patient performed finger-tapping movements to identify hand area of the primary motor cortex (see Methods). The results of these two scans are shown in Figure 3B. In contrast to the consistency of the resting state maps in Figure 3A, the task-based maps showed much more variability in functional localization, primarily within the lesion-distorted cortex. A band of activation within the tumor was present in trial 2 (Figure 3B, right panel, blue arrows), but absent in trial 1 (Figure 3B, left panel). This band of activation, in fact, encompassed a region larger in volume than the activation anterior-lateral to the tumor, which likely represents the true location of the sensorimotor system in the right hemisphere. Intraoperatively, a complete resection was performed with the aid of CSM which included removal of the tumor tissue that showed activation with task-based fMRI. Postoperatively, the patient exhibited only mild left-sided weakness, suggesting that the activation within the tumor was likely artifactual. Histological exam revealed the mass to be a glioblastoma multiforme (GBM).

Case 2

A 54-year-old female was admitted for treatment of metastatic melanoma. One year earlier she underwent Gamma Knife therapy for a right parietal metastatic lesion. Tumor progression manifested as weakness of the left leg. Structural MRI showed enlargement of a right parietal lesion (Figure 4A). Task-based fMRI using the finger-tapping paradigm failed for unknown reasons (Figure 4B). Resting state functional localization revealed anterior and lateral shift of the sensorimotor network in the ipsilateral hemisphere (Figure 4C). No CSM data were available from this case.

Case 3

A 64-year-old male presented with a several-week history of focal motor seizures involving his right lower extremity. Structural MR demonstrated a 3cm rim-enhancing heterogeneous mass in the left frontoparietal area adjacent to the postcentral gyrus (Figure 5A). Finger-tapping fMRI revealed a pattern of activity around the central sulcus in both hemispheres, shifted slightly anteriorly but otherwise resembling the sensorimotor network. However, a large band of activity also was present in the right parietal cortex, not consistent with the typical sensorimotor localization topography (Figure 5B). Resting state mapping dissociated the activations into two networks. Seeding the hemisphere contralateral to the tumor produced correlations with motor cortex in the ipsilateral hemisphere (Figure 5C). The resting-state sensorimotor correlations were anteriorly shifted bilaterally in a manner similar to the task-evoked activations. Blind source separation of the resting state data using independent component analysis (ICA) separately confirmed the presence of this anteriorly shifted network (Figure 5D). A second and separable resting state network was identified matching the topography of the parietal pattern of activation from the task-evoked scan (Figure 5E). This parietal pattern is similar in spatial organization and localization to the dorsal attention network (10, [16]). Cortical stimulation elicited hand movement near the lateral anterior border of the tumor (Figure 5A, green circle). This area on the cortical surface was adjacent to activity in

both the resting state and task-based maps, although sensorimotor specificity was greater in the resting state map. Post resection pathology indicated a GBM.

Case 4

A 57-year-old female with a history of Graves' disease presented with weakness of the left arm. Structural MRI showed a heterogeneous, ring-enhancing lesion located just anterior to the medial right precentral gyrus with surrounding edema (Figure 6A). Postoperative histopathology showed GBM. Task-evoked fMRI mapping showed activation around the central sulcus in both hemispheres, as well as multiple foci in left hemisphere extending posteriorly to parts of parietal cortex (Figure 6B). The tumor did not appear to have extensively disrupted the sensorimotor network in this patient, although a slight shift in cortical tissue posterior to the tumor may have been present. Resting state mapping revealed correlated activity around the central sulcus in both hemispheres in a distribution typical of the sensorimotor system (Figure 6C). Intraoperative cortical mapping showed evoked hand responses with stimulation postero-lateral to the tumor (Figure 6A, green circle), consistent with task-evoked and resting state activity.

Separation of Sensory and Motor Activity

So far, the results presented have delineated a single network that includes both motor and sensory components. This finding is consistent with previous resting state studies showing high coherence within the sensorimotor network using a variety of methodologies (3,[7],[18]). In a neurosurgical setting, segregation of these two cortices is desirable when this information can help minimize the degree of neurological deficits post-resection. Therefore, we pursued a method to separate motor and sensory activity. Even though these two cortices show a high degree of correlated activity, they are not perfectly synchronous. This observation led us to ask whether the activity *unique* to either cortex would generate a more precise map localized to either the precentral sulcus or the postcentral sulcus. To answer this question, we created representative ROIs restricted to either the motor or sensory cortex and used partial correlation to eliminate the shared variance between the two ROIs prior to generating correlation maps. Results are shown in Figure 7 for two representative patients (Cases 2 and 4). Motor/sensory separation is seen near the seed regions, as expected. More importantly, in the contralateral hemisphere motor and sensory activity also segregated along the central sulcus even when the tumor distorted local morphology (Figure 7, blue box).

Discussion

The purpose of this study was to demonstrate an initial experience with resting state correlation mapping for functional localization in patients with brain tumors. In our case series we found that the spatial localization of sensorimotor cortex using resting state correlation mapping compared well with localization using “gold standard” intraoperative cortical stimulation mapping. Resting state correlation proved to be a reliable method that produced consistent maps over multiple scans. Our preliminary observations suggest that this method may be less variable than maps obtained with a standard task-based fMRI protocol. Resting state analysis revealed specificity of correlations within the sensorimotor network even when task-based fMRI showed multiple cortical systems correlated with the task. Finally, functional localization can be achieved even when the task-based method fails (as in Case 2) or when the patient is unable to perform the task. These findings demonstrate the utility of resting state correlation mapping as a potential tool for preoperative functional localization though this limited case series needs to be expanded before definitive conclusions can be drawn.

Reproducibility of Resting State Maps

Previously published work have shown the consistency of the sensorimotor network at a group level which is supports our current findings but we extend this analysis to the individual level (13). Figure 1B shows that correlated activity reproducibly appears within the sensorimotor system in *single individuals* scanned multiple times, thereby demonstrating the reliability of this method for individual patient use. Furthermore, correlation maps within an individual are more similar than across individuals, suggesting that resting state mapping is sensitive enough to capture a portion of the individual variability seen in a group of subjects. In Case 1 Figure 3, task-based fMRI mapping with a standard protocol used in the clinic showed more variability than the resting state maps, but acquisition times varied between the two maps (4 minutes for task vs. 15 minutes for resting state). A definitive comparison of the two methods will need to include equal acquisition times performed within a larger patient population for statistical testing. Our results in a large population of healthy adults show that consistent resting state maps can be generated in 7 minutes or less with a 3T scanner. Optimal scanning time remains to be determined especially in a patient population where head motion may be a greater contributing factor than in healthy adults. Acquisition times for task-based fMRI may need to be increased from the present typical 4 minutes to generate meaningful activation maps given the variability seen in the two Case 1 trials (Figure 3A).

Versatility of Resting State Mapping

Perhaps more importantly, there are many patient factors such as mental status change, immaturity, dementia, delirium, aphasia, and deafness that preclude the use of task-based fMRI, denying its potential benefits to a wide range of patients. Resting state correlation mapping offers a definitive advantage in these instances, as illustrated in Case 2. Though task-based mapping was unsuccessful in this patient, resting state analysis showed clear localization to the sensorimotor cortex. Previously reported results have shown that resting state localization is achievable even during sleep and under the effects of general anesthesia (29, [30,36,44]). Patients with uncontrollable head motion and young children, who are often more prone to restlessness, stand to benefit from resting state scans under anesthesia.

Comparison with CSM

Having established the consistency and potential utility of this method in a broad patient population, the accuracy of resting state mapping was tested against CSM, the “gold standard” for intraoperative functional identification. In all three cases where CSM data were available, the two methods agreed allowing for technical imprecision: CSM current is applied to the pial surface whereas the hemodynamic response is measured in gray matter extending over gyri and sulci. Resting state correlation mapping may prove useful not only for preoperative planning and assessment of risk but also intraoperatively when integrated into neuronavigation tools during tumor and epilepsy resections.

Integration and Segregation of Sensory and Motor Activity

Strong correlated activity between motor and sensory cortex is not a finding unique to resting state mapping but generalize to other modalities such as traditional task-evoked fMRI. Even a simple finger-tapping exercise generates activation that spans across the central sulcus, presumably through sensory feedback during voluntary movement (see Figures 3A, 6B for examples). This coherence is expected, though, given the indispensible need for functional interaction between input and output and the co-evolution of the two adjacent systems to produce strong anatomical interconnections. Nevertheless, our partial correlation results demonstrate that motor and sensory cortices possess measurable signatures of neuronal activity that are unique and separable. Activity unique to each system is correlated across hemispheres and can be exploited for presurgical localization in tumor-lesioned tissue.

Other Resting State Networks

We confined our report to the sensorimotor network to achieve a homogeneous case series and to exploit comparison with CSM. However, with the same resting state dataset it is possible to functionally characterize the spatial organization of other functional networks that may be of importance. Previous studies have described various networks that can be seen in the resting state, including the language network, hippocampal-parietal memory network, default network, dorsal and ventral attention network, control network, and the thalamocortical network, all of which may be applicable for expanded presurgical planning (16,[22],[27],[43],[45],[49]). The utility of characterizing multiple networks was demonstrated in Case 3. Task-based fMRI revealed a spatial pattern uncharacteristic of the normal sensorimotor network (Figure 5B) in the right intraparietal sulcus, which is typically a component of the dorsal attention system (10,[16]). By placing a seed in the sensorimotor network and the intraparietal sulcus (IPS), resting state mapping was able to tease these two networks apart (Figure 5C,E). Thus, resting state correlation mapping is capable of improved specificity as compared to task-based fMRI. As a general principle, this case revealed that the operational differences between analytic techniques based on task performance and those based on the intrinsic activity of the brain can generate two very different results. If the goal is to specifically localize one neuroanatomical system, then resting state mapping may offer an advantage over task-based fMRI.

Seed-based Mapping and ICA

Case 3 represents a unique example of functional reorganization in both the tumor-lesioned and the morphologically normal hemisphere. Seed placement was shifted anteriorly to capture the displaced sensorimotor network, which was similarly displaced in task activation map. In cases where functional reorganization occurs and task activation cannot serve as a guide for seed placement, resting state mapping approaches using ICA would be beneficial in localizing a sensorimotor network with altered topography. Blind source separation using ICA does not rely on *a priori* seeding thus eliminating operator variability when a standardized seed in sensorimotor network cannot be used. With ICA, the spatial-temporal fMRI signal is separated into independent components (ICs) by optimizing for maximally independent spatial sources (3). The result of such an analysis features multiple ICs, each separated into a spatially distinct grouping of voxels, some of which represent resting state networks such as the sensorimotor system, and some of which represent spurious variance such as vascular artifacts, movement artifacts, and machine noise.

In the majority of cases, seed-based mapping efficiently maps the sensorimotor system without the need, as with ICA, to manually sift through numerous ICs for each case (126 ICs for Case 3) which would be suboptimal in a neurosurgical setting. In this sense, seed-based mapping and ICA can be seen as complementary tools for resting state mapping, each with a set of advantages depending on the specific clinical case.

Limitations

While the current work demonstrates great promise, there are existing limitations to overcome. Automatic quality control steps should be performed to check registration precision of the patient's structural MRI with standard anatomical space. In cases of severe anatomic distortions due to tumor effects, non-linear transformations may be preferable to linear.

A goodness of fit criterion should be used to specify whether a standardized seed region adequately captures the sensorimotor network. A potential implementation of such a criterion would be the creation of a template map of the sensorimotor system. Testing should ideally be conducted in a large group of patients to generate the appropriate statistical thresholds for goodness of fit.

Future Directions

Future studies will focus on a larger patient population with more complete intraoperative functional localization of the cortex. The scope of functional localization can also be expanded in future studies from the present application in sensorimotor cortex to other cortical networks such as the language network where resting state correlation mapping may offer a distinct advantage over intraoperative cortical mapping for localizing intrasulcal language areas inaccessible with cortical stimulation. We recognize that localization of the language network is more anatomically variable than sensorimotor localization (40). In such pursuits, ICA may be the preferred method of resting state network delineation. Previous studies hint that lateralization may be present in the language network at rest (27). This phenomenon, obviously important in a neurosurgical setting, remains to be investigated. Definitive verification of the topography of resting state networks devoted to higher cortical function will likely come from the combination of diverse measurements such as neuroanatomical tracing/imaging of structural connections, resting state imaging, and task-evoked imaging during engagement and performance of these higher cognitive functions (44).

An important avenue for future work will be determining how best to combine task-based and resting state mapping for optimal pre-operative functional localization. Ideally, one would like to perform both task-based and resting state runs to take advantage of the strengths of each method. However, in clinical practice with constraints on scanner time and patient tolerance this may prove difficult. One useful solution may be to use apply both processing techniques to the same data. Recent work has suggested an approximately linear superposition between spontaneous fluctuations and task related modulations in fMRI data (2,[20]). Given this finding, it may be possible to remove task-related modulation from task data to obtain results similar to resting state correlation mapping (15). Applying these principals to pre-operative mapping, one could acquire task data with minimal acquisition time then process the data in two ways: once to obtain task-activation maps and seed regions and a second time to obtain resting state correlation maps. The two maps could then be combined using a flexible weighting scheme based on the robustness of the two maps in each particular patient. Such an approach could optimize pre-operative functional localization across a wide range of patients with no additional investment in scanner time.

More generally, the utility of preoperative functional mapping to neurosurgical planning will need to be evaluated in terms of benefits for post-operative functional outcome and survival. Power in preoperative assessment potentially may be increased with the combination of functional imaging with structural imaging methods such as diffusion weighted imaging. Much progress has been made in the quality of fiber tract reconstruction using probabilistic methods of estimating the diffusion tensor model and in model free reconstructions with diffusion spectrum imaging (4,[26]). Such integrative studies would be best suited to answering questions of functional relationships and anatomical pathways contributing to functional synchrony. Other methods such as intrinsic optical imaging represent a promising technique for rapid high resolution intraoperative localization of neuronal activity on the cortical surface (23,[25],[41]). To improve registration of preoperative images with intraoperative neuronavigation systems, laser scanning and intraoperative structural MRI can be performed to correct for non-linear effects caused by brain shift after skull removal. Other interesting avenues of investigation include the impact of neuronal migrational disorders and cortical dysplasia on mosaicism and atypical functional localization of eloquence, as confirmed with gold standard CSM and validated by resting stage correlation mapping; as well as the utility of resting stage correlation mapping on preoperative planning for cortical epilepsy surgery.

Conclusions

In this report there are several findings critical for evaluation of resting state correlation mapping as a potential aid in the neurosurgical planning of brain tumor resections. Consistency of the method was demonstrated both within a group of healthy individuals and a case series of patients with brain tumors. We provide evidence supporting accurate localization of the sensorimotor system by comparison with intraoperative cortical stimulation mapping. A clear advantage of the method over task-based fMRI is that it can be performed in a wide range of patients that are not candidates for task-based fMRI because of sedation or young age. Another advantage is that a single scan offers the ability to image functional relationships among all brain areas, producing maps of various neuronal networks. Lastly, resting state scans can be easily appended to standard pre-operative structural MR protocols with minimal increase in total acquisition time, thereby making implementation feasible in most clinical settings.

Acknowledgments

Financial Support: This work was supported by NIH NS06833 (MER); NIMH F30MH083483 (DZ); NIH K23 HD053212 (JSS); the Mallinkrodt Institute of Radiology Start up funds; Grant Number UL1 RR024992 from the National Center for Research Resources (NCRR), a component of the National Institutes of Health (NIH), and NIH Roadmap for Medical Research. Its contents are solely the responsibility of the authors and do not necessarily represent the official view of NCRR or NIH.

References

1. Adcock JE, Wise RG, Oxbury JM, Oxbury SM, Matthews PM. Quantitative fMRI assessment of the differences in lateralization of language-related brain activation in patients with temporal lobe epilepsy. Neuroimage 2003;18:423–438. [PubMed: 12595196]
2. Arfanakis K, Cordes D, Haughton VM, Moritz CH, Quigley MA, Meyerand ME. Combining independent component analysis and correlation analysis to probe interregional connectivity in fMRI task activation datasets. Magn Reson Imaging 2000;18:921–930. [PubMed: 11121694]
3. Beckmann CF, DeLuca M, Devlin JT, Smith SM. Investigations into resting-state connectivity using independent component analysis. Philosophical transactions of the Royal Society of London 2005;360:1001–1013. [PubMed: 16087444]
4. Behrens TE, Woolrich MW, Jenkinson M, Johansen-Berg H, Nunes RG, Clare S, Matthews PM, Brady JM, Smith SM. Characterization and propagation of uncertainty in diffusion-weighted MR imaging. Magn Reson Med 2003;50:1077–1088. [PubMed: 14587019]
5. Binder JR, Swanson SJ, Hammeke TA, Morris GL, Mueller WM, Fischer M, Benbadis S, Frost JA, Rao SM, Haughton VM. Determination of language dominance using functional MRI: a comparison with the Wada test. Neurology 1996;46:978–984. [PubMed: 8780076]
6. Biswal B, Yetkin F, Haughton V, Hyde J. Functional connectivity in the motor cortex of resting human brain using echo-planar MRI. Magnetic Resonance in Medicine 1995;34:537–541. [PubMed: 8524021]
7. Biswal B, Yetkin FZ, Haughton VM, Hyde JS. Functional connectivity in the motor cortex of resting human brain using echo-planar MRI. Magn Reson Med 1995;34:537–541. [PubMed: 8524021]
8. Boynton GM, Engel SA, Glover GH, Heeger DJ. Linear systems analysis of functional magnetic resonance imaging in human V1. J Neurosci 1996;16:4207–4221. [PubMed: 8753882]
9. Corbetta M, Kincade JM, Shulman GL. Neural systems for visual orienting and their relationships to spatial working memory. J Cogn Neurosci 2002;14:508–523. [PubMed: 11970810]
10. Corbetta M, Shulman GL. Control of goal-directed and stimulus-driven attention in the brain. Nature reviews 2002;3:201–215.
11. Cordes D, Haughton VM, Arfanakis K, Wendt GJ, Turski PA, Moritz CH, Quigley MA, Meyerand ME. Mapping functionally related regions of brain with functional connectivity MR imaging. American Journal of Neuroradiology 2000;21:1636–1644. [PubMed: 11039342]

12. Cordes D, Haughton VM, Arfanakis K, Wendt GJ, Turski PA, Moritz CH, Quigley MA, Meyerand ME. Frequencies contributing to functional connectivity in the cerebral cortex in 'resting-state' data. American Journal of Neuroradiology 2001;22:1326–1333. [PubMed: 11498421]
13. Damoiseaux JS, Rombouts SA, Barkhof F, Scheltens P, Stam CJ, Smith SM, Beckmann CF. Consistent resting-state networks across healthy subjects. Proc Natl Acad Sci U S A 2006;103:13848–13853. [PubMed: 16945915]
14. De Luca M, Smith SM, De Stefano N, Federico A, Matthews PM. Blood oxygenation level dependent contrast resting state networks are relevant to functional activity in the neocortical sensorimotor system. Experimental Brain Research 2005;167:587–594.
15. Fair DA, Schlaggar BL, Cohen AL, Miezin FM, Dosenbach NU, Wenger KK, Fox MD, Snyder AZ, Raichle ME, Petersen SE. A method for using blocked and event-related fMRI data to study "resting state" functional connectivity. Neuroimage 2007;35:396–405. [PubMed: 17239622]
16. Fox MD, Corbetta M, Snyder AZ, Vincent JL, Raichle ME. Spontaneous neuronal activity distinguishes human dorsal and ventral attention systems. Proc Natl Acad Sci U S A 2006;103:10046–10051. [PubMed: 16788060]
17. Fox MD, Raichle ME. Spontaneous fluctuations in brain activity observed with functional magnetic resonance imaging. Nat Rev Neurosci 2007;8:700–711. [PubMed: 17704812]
18. Fox MD, Snyder AZ, Vincent JL, Corbetta M, Van Essen DC, Raichle ME. The human brain is intrinsically organized into dynamic, anticorrelated functional networks. Proc Natl Acad Sci U S A 2005;102:9673–9678. [PubMed: 15976020]
19. Fox MD, Snyder AZ, Vincent JL, Raichle ME. Intrinsic fluctuations within cortical systems account for intertrial variability in human behavior. Neuron 2007;56:171–184. [PubMed: 17920023]
20. Fox MD, Snyder AZ, Zacks JM, Raichle ME. Coherent spontaneous activity accounts for trial-to-trial variability in human evoked brain responses. Nature Neuroscience 2006;9:23–25.
21. Fukunaga M, Horovitz SG, Van Gelderen P, de Zwart JA, Jansma JM, Ikonomidou VN, Chu R, Deckers RHR, Leopold DA, Duyn JH. Large-amplitude, spatially correlated fluctuations in BOLD fMRI signals during extended rest and light sleep. Magnetic resonance imaging 2006;24:979–992. [PubMed: 16997067]
22. Greicius MD, Krasnow B, Reiss AL, Menon V. Functional connectivity in the resting brain: a network analysis of the default mode hypothesis. Proc Natl Acad Sci U S A 2003;100:253–258. [PubMed: 12506194]
23. Grinvald A, Lieke E, Frostig RD, Gilbert CD, Wiesel TN. Functional architecture of cortex revealed by optical imaging of intrinsic signals. Nature 1986;324:361–364. [PubMed: 3785405]
24. Haberg A, Kvistad KA, Unsgard G, Haraldseth O. Preoperative blood oxygen level-dependent functional magnetic resonance imaging in patients with primary brain tumors: clinical application and outcome. Neurosurgery 2004;54:902–914. discussion 914-905. [PubMed: 15046657]
25. Haglund MM, Ojemann GA, Hochman DW. Optical imaging of epileptiform and functional activity in human cerebral cortex. Nature 1992;358:668–671. [PubMed: 1495561]
26. Hagmann P, Jonasson L, Maeder P, Thiran JP, Wedeen VJ, Meuli R. Understanding diffusion MR imaging techniques: from scalar diffusion-weighted imaging to diffusion tensor imaging and beyond. Radiographics 2006;26(Suppl 1):S205–223. [PubMed: 17050517]
27. Hampson M, Peterson BS, Skudlarski P, Gatenby JC, Gore JC. Detection of functional connectivity using temporal correlations in MR images. Human Brain Mapping 2002;15:247–262. [PubMed: 11835612]
28. Horovitz, SG.; Fukunaga, M.; de Zwart, JA.; Van Gelderen, P.; Fulton, SC.; Balkin, TJ.; Duyn, JH. The default-mode network connectivity during awake and early sleep,: A simultaneous EEG-BOLD-fMRI study. Organization for Human Brain Mapping Annual Meeting; Florence, Italy. 2006. M-PM
29. Johnston JM, Vaishnavi SN, Smyth MD, Zhang D, He BJ, Zempel JM, Shimony JS, Snyder AZ, Raichle ME. Loss of resting interhemispheric functional connectivity after complete section of the corpus callosum. J Neurosci 2008;28:6453–6458. [PubMed: 18562616]
30. Kiviniemi V, Kantola JH, Jauhiainen J, Hyvarinen A, Tervonen O. Independent component analysis of nondeterministic fMRI signal sources. NeuroImage 2003;19:253–260. [PubMed: 12814576]

31. Lee CC, Ward HA, Sharbrough FW, Meyer FB, Marsh WR, Raffel C, So EL, Cascino GD, Shin C, Xu Y, Riederer SJ, Jack CR Jr. Assessment of functional MR imaging in neurosurgical planning. AJNR Am J Neuroradiol 1999;20:1511–1519. [PubMed: 10512239]
32. Lemieux L. Electroencephalography-correlated functional MR imaging studies of epileptic activity. Neuroimaging Clin N Am 2004;14:487–506. [PubMed: 15324860]
33. Logothetis NK. The underpinnings of the BOLD functional magnetic resonance imaging signal. Journal of Neuroscience 2003;23:3963–3971. [PubMed: 12764080]
34. Lowe MJ, Mock BJ, Sorenson JA. Functional connectivity in single and multislice echoplanar imaging using resting-state fluctuations. NeuroImage 1998;7:119–132. [PubMed: 9558644]
35. Matthews PM, Honey GD, Bullmore ET. Applications of fMRI in translational medicine and clinical practice. Nat Rev Neurosci 2006;7:732–744. [PubMed: 16924262]
36. Peltier SJ, Kerssens C, Hamann SB, Sebel PS, Byas-Smith M, Hu X. Functional connectivity changes with concentration of sevoflurane anaesthesia. Neuroreport 2005;16:285–288. [PubMed: 15706237]
37. Pujol J, Conesa G, Deus J, Lopez-Obarrio L, Isamat F, Capdevila A. Clinical application of functional magnetic resonance imaging in presurgical identification of the central sulcus. J Neurosurg 1998;88:863–869. [PubMed: 9576255]
38. Raichle, ME. A brief history of human functional brain mapping. In: Toga, AW.; Mazziotta, JC., editors. Brain Mapping The Systems. San Diego: Academic Press; 2000. p. 33-75.
39. Raichle ME, Mintun MA. Brain work and brain imaging. Annual Review of Neuroscience 2006;29:449–476.
40. Sanai N, Mirzadeh Z, Berger MS. Functional outcome after language mapping for glioma resection. N Engl J Med 2008;358:18–27. [PubMed: 18172171]
41. Sato K, Nariai T, Sasaki S, Yazawa I, Mochida H, Miyakawa N, Momose-Sato Y, Kamino K, Ohta Y, Hirakawa K, Ohno K. Intraoperative intrinsic optical imaging of neuronal activity from subdivisions of the human primary somatosensory cortex. Cereb Cortex 2002;12:269–280. [PubMed: 11839601]
42. Smith SM, Jenkinson M, Woolrich MW, Beckmann CF, Behrens TE, Johansen-Berg H, Bannister PR, De Luca M, Drobnjak I, Flitney DE, Niazy RK, Saunders J, Vickers J, Zhang Y, De Stefano N, Brady JM, Matthews PM. Advances in functional and structural MR image analysis and implementation as FSL. Neuroimage 2004;23(Suppl 1):S208–219. [PubMed: 15501092]
43. Vincent JL, Kahn I, Snyder AZ, Raichle ME, Buckner RL. Evidence for a Frontoparietal Control System Revealed by Intrinsic Functional Connectivity. J Neurophysiol. 2008
44. Vincent JL, Patel GH, Fox MD, Snyder AZ, Baker JT, Van Essen DC, Zempel JM, Snyder LH, Corbetta M, Raichle ME. Intrinsic functional architecture in the anesthetized monkey brain. Nature 2007;447:83–86. [PubMed: 17476267]
45. Vincent JL, Snyder AZ, Fox MD, Shannon BJ, Andrews JR, Raichle ME, Buckner RL. Coherent spontaneous activity identifies a hippocampal-parietal memory network. J Neurophysiol 2006;96:3517–3531. [PubMed: 16899645]
46. Vlieger EJ, Majoie CB, Leenstra S, Den Heeten GJ. Functional magnetic resonance imaging for neurosurgical planning in neurooncology. Eur Radiol 2004;14:1143–1153. [PubMed: 15148622]
47. Xiong J, Parsons LM, Gao JH, Fox PT. Interregional connectivity to primary motor cortex revealed using MRI resting state images. Human Brain Mapping 1999;8:151–156. [PubMed: 10524607]
48. Zacks JM, Braver TS, Sheridan MA, Donaldson DI, Snyder AZ, Ollinger JM, Buckner RL, Raichle ME. Human brain activity time-locked to perceptual event boundaries. Nat Neurosci 2001;4:651–655. [PubMed: 11369948]
49. Zhang D, Snyder AZ, Fox MD, Sansbury MW, Shimony JS, Raichle ME. Intrinsic Functional Relations between Human Cerebral Cortex and Thalamus. J Neurophysiol. 2008
50. Zhang D, Snyder AZ, Fox MD, Sansbury MW, Shimony JS, Raichle ME. Intrinsic functional relations between human cerebral cortex and thalamus. J Neurophysiol 2008;100:1740–1748. [PubMed: 18701759]

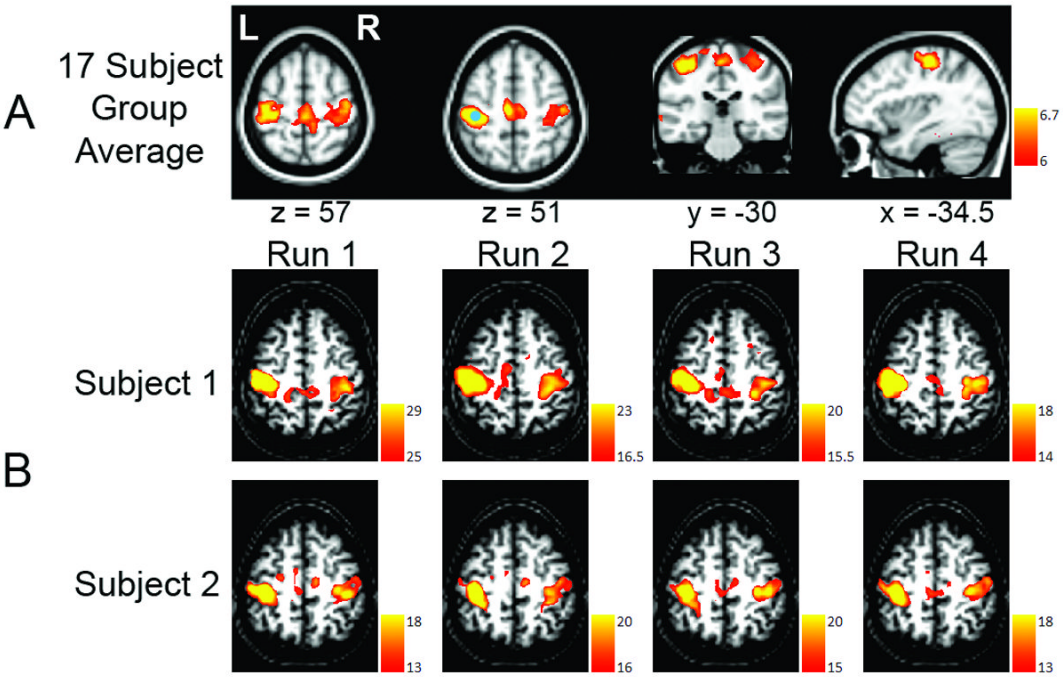

Figure 1.

Resting state correlation maps showing the distribution of the sensorimotor network in normal subjects. A: The average correlation map in a group of 17 healthy young adults. The bilateral pattern represents correlated neuronal activity between left and right sensorimotor cortices. Seed placement is shown by the blue circle. B: The consistency of resting state correlation mapping is demonstrated by repeated scans in single subjects. Four 7 minute scans were performed in each of the 17 subjects. Two subjects are displayed here showing the correlation map from each of the four scans (transverse slices, z=51). Correlations contralateral to the seed are consistently seen in the same region within the sensorimotor network in each of the repeated scans. All images are displayed left-on-left (neurologic convention).

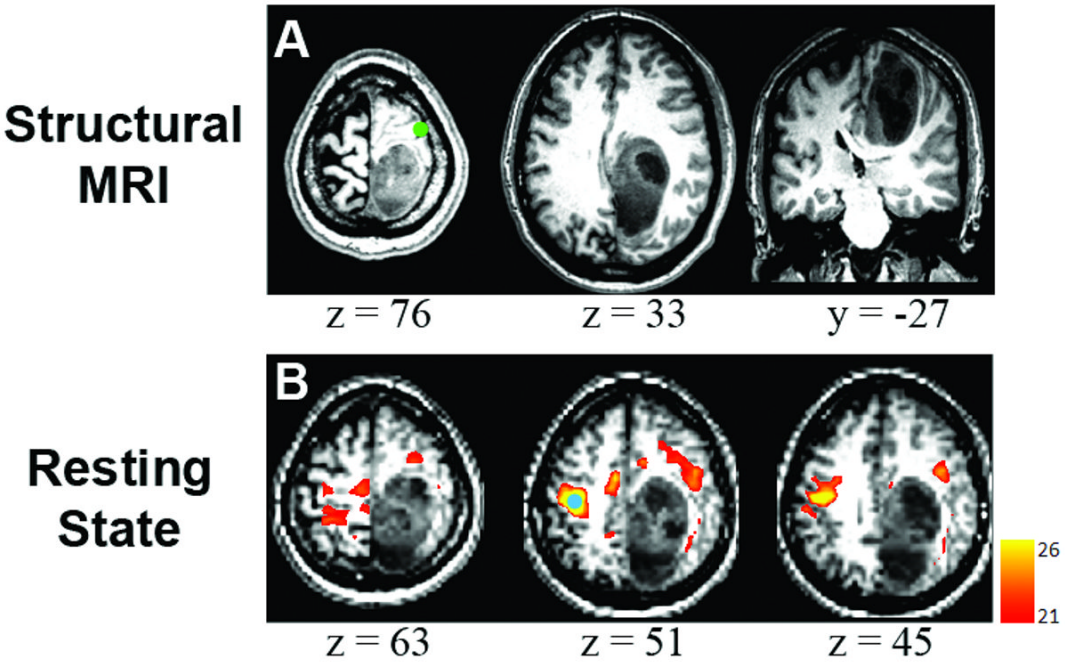

Figure 2.

Case 1. A: Structural MRI showing the location of the tumor which primarily disrupts right parietal, somatosensory and motor cortices (neurologic convention). The green circle represents the location of ipsilateral hand response to cortical stimulation. B: Resting state correlation map showing the distribution of the sensorimotor network in this patient. A seed was placed in the sensorimotor cortex of the contralateral hemisphere (blue circle). Correlations in the ipsilateral hemisphere were predominantly localized to a region anterior and lateral to the tumor, displaced by the intracranial mass. All images are displayed left-on-left (neurologic convention).

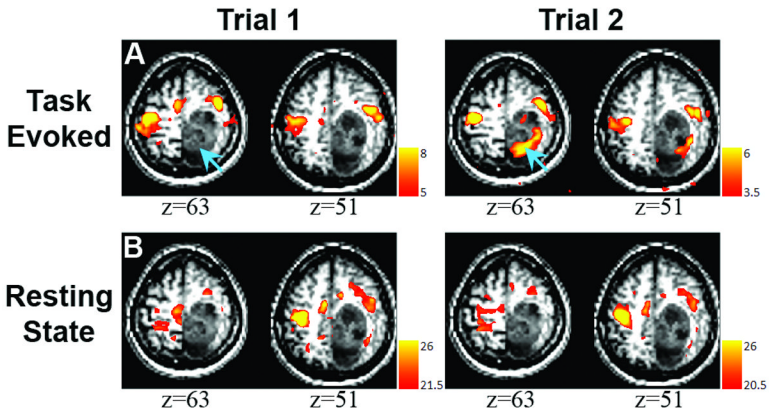

Figure 3.

Comparison of resting state and task-related fMRI mapping in Case 1. A: Finger-tapping fMRI × 2. Activity within the tumor (blue arrows) was seen in trial 2 but not in trial 1. B: Resting state correlation mapping × 2 shows a similar distribution of correlated activity, resembling the activation from trial 1 but not trial 2 of the task. All images are displayed left-on-left (neurologic convention).

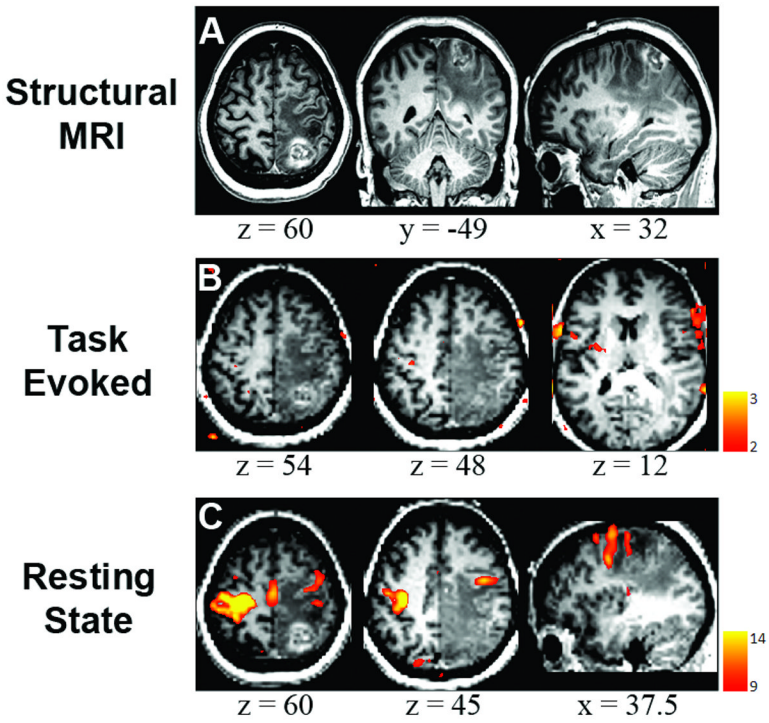

Figure 4.

Case 2. A: Structural MRI revealed a tumor in right parietal cortex extending anteriorly into motor and somatosensory areas (neurologic convention). B: Task-related fMRI failed to reveal activity within the sensorimotor cortex. A deliberately low threshold reveals noise outside of the brain without responses within the sensorimotor network. C: Resting state correlation mapping using a seed in contralateral hemisphere (same seed as in Figure 2B, blue circle) showed that ipsilateral sensorimotor cortex near the tumor was displaced anteriorly and laterally. All images are displayed left-on-left (neurologic convention).

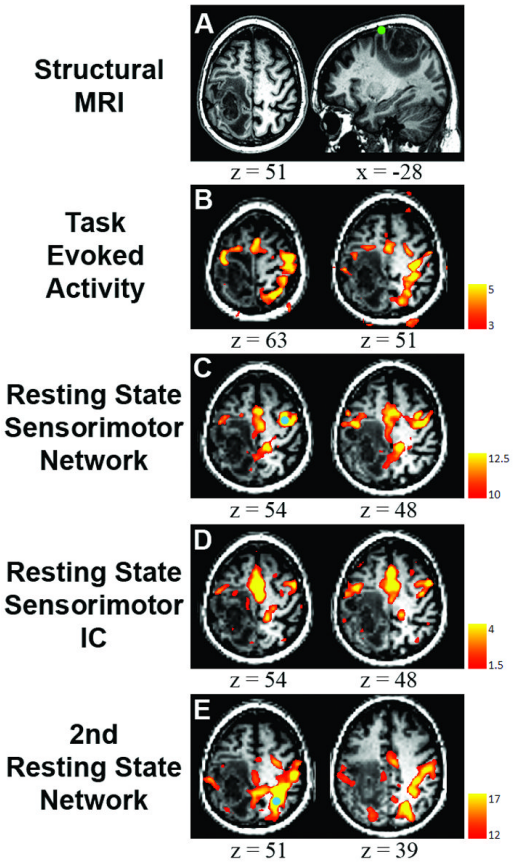

Figure 5.

Case 3. A: Structural MRI revealed a tumor in left parietal cortex that invades territory near the central sulcus (neurologic convention). The green circle represents the location of ipsilateral hand response to cortical stimulation. B: Task-related activity was seen bilaterally in frontal lobe. In addition, a large band of activity appeared in right parietal cortex, not consistent with the pattern of activity from the sensorimotor network. C: Resting state correlation mapping using a seed in the right (unaffected) hemisphere (blue circle) showed ipsilateral correlations anterior to the tumor as well as a region of activity in midline parietal cortex. Note absence in the correlation mapping results of parietal activity seen in the task-related map. D: ICA decomposition is an alternative method that does not rely on *a priori* seed placement. Results from ICA verify the anterior shift of the sensorimotor network. E. Parietal activation seen during task-evoked scan is revealed to be a separate resting state network that is normally dissociated from the sensorimotor network (seed: blue circle). All images are displayed left-on-left (neurologic convention).

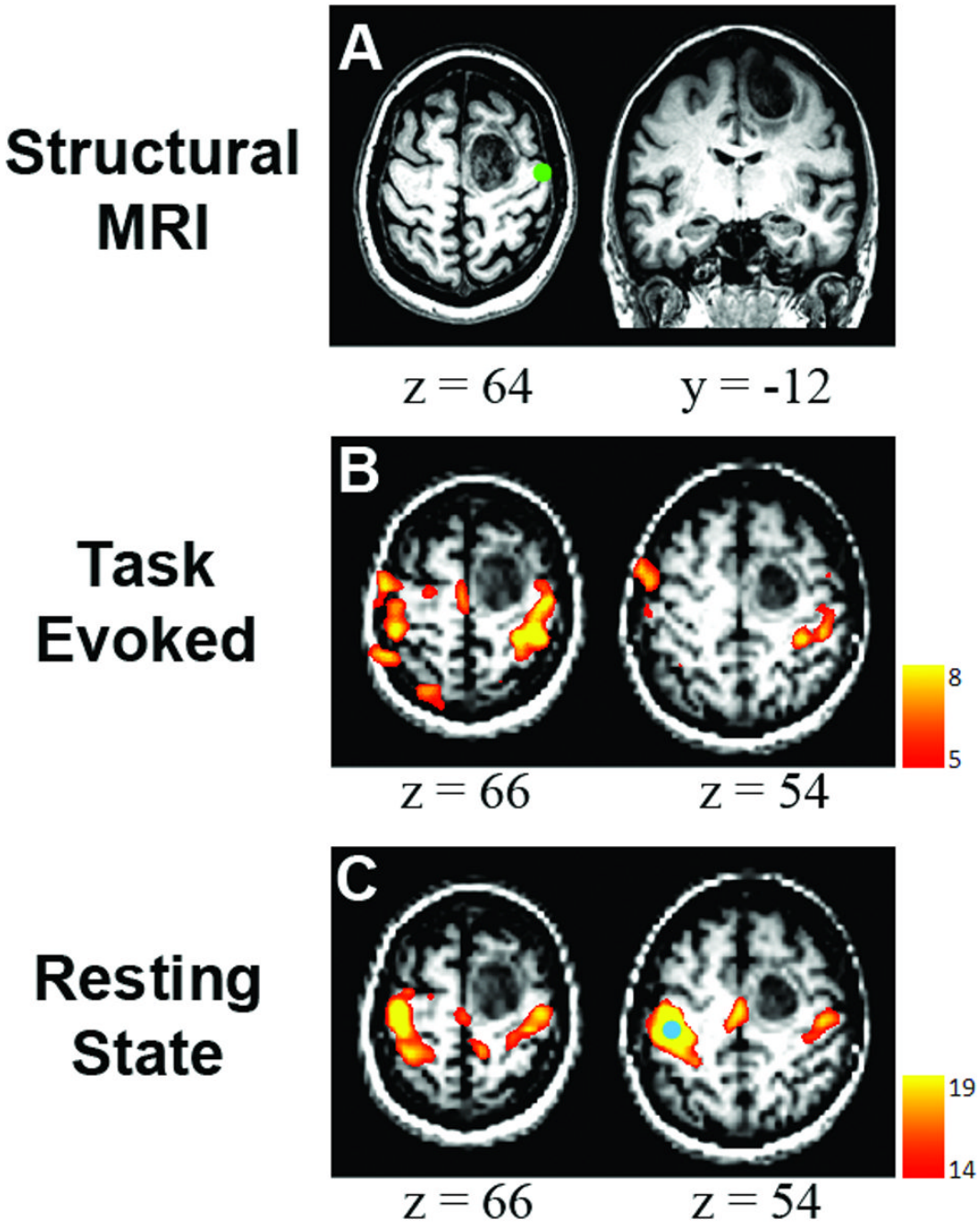

Figure 6.

Case 4. A: Structural MRI showed a mass in right frontal cortex (neurologic convention). The green circle represents the location of ipsilateral hand response to cortical stimulation. B: Task-related mapping shows activity within the sensorimotor network but also small responses in parietal cortex that are seemingly unrelated to motor function or sensation. C: Resting state correlation mapping showed that the sensorimotor network was largely unaffected by the tumor anterior to the central sulcus. The seed region is marked by the blue circle. All images are displayed left-on-left (neurologic convention).

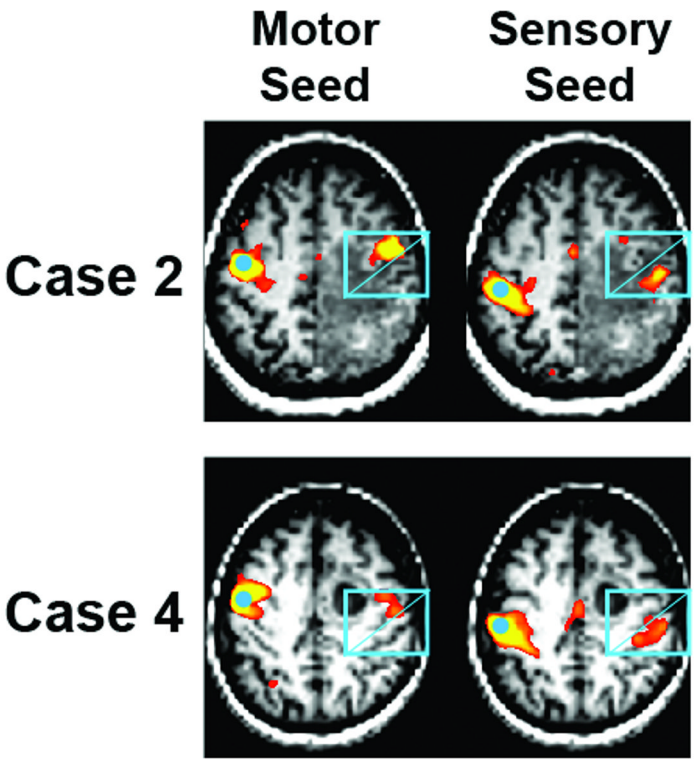

Figure 7.

Separation of Sensory and Motor Activity. Motor and sensory cortices exhibit highly correlated neuronal activity. Separation of activity unique to each area can be achieved using partial correlation. Two seeds are defined, representing motor and sensory cortex (blue circles). Partial correlation eliminates activity that is shared between the two ROIs before correlation maps are computed. Shown for two representative cases, correlations contralateral to the seeds (blue box) can be seen to segregate along the central sulcus. The location and angle of the central sulcus is approximated by the blue diagonal. All images are displayed left-on-left (neurologic convention).

Table 1

Case Number	Age/Sex	Presurgical Neurological Exam Status	Tumor Location	Histopathology
1	57/M	normal	R parietal, motor, somatosensory	Glioblastoma multiforme
2	54/F	L LE weakness	R parietal, motor, somatosensory	Metastatic melanoma
3	64/M	mild R UE and LE weakness	L posterofrontal/parietal cortex	Glioblastoma multiforme
4	57/F	normal	R frontal cortex anterior to precentral gyrus	Glioblastoma multiforme